

Supporting Information

UV-Crosslinkable Graphene/ poly (trimethylene carbonate) Composites for 3D Printing of Electrically Conductive Scaffolds

Sepidar Sayyar[†], Miina Bjorninen[†], Suvi Haimi^{‡§}, Susanna Miettinen^{||}, Kerry Gilmore[†], Dirk Grijpma^{§#}, Gordon Wallace^{†}*

[†]ARC Centre of Excellence for Electromaterials Science (ACES), Intelligent Polymer Research Institute, AIIM Facility, Innovation Campus, University of Wollongong, NSW 2522, Australia

[‡]Department of Oral and Maxillofacial Sciences, Clinicum, University of Helsinki Helsinki, Finland

[§]MIRA Institute for Biomedical Technology and Technical Medicine, Department of Biomaterials Science and Technology, University of Twente, Enschede, The Netherlands.

^{||}Adult Stem Cell Group, BioMediTech, University of Tampere, Tampere, Finland

[#]Department of Biomedical Engineering, University of Groningen, University Medical Center Groningen, Groningen, The Netherlands

*E-mail: gwallace@uow.edu.au

The following document presents further work and clarification of synthesis and characterization of UV-crosslinkable graphene/ poly(trimethylene carbonate) composites.

Differential Scanning Calorimetry

The PTMC macromer has a melting point of $\sim 38^{\circ}\text{C}$ and a T_g of $\sim -20^{\circ}\text{C}$ (**Figure S 1**). The latter increased slightly to -15°C after crosslinking. No melting point could be observed after crosslinking the PTMC, which confirmed formation of crosslinks between the macromolecules that prevented the mobility of the polymer chains. Addition of graphene barely changed the T_g of the polymer, the PTMC with 3 wt.% CCG showed a T_g of around -16°C . There is no melting peak in the sample with 3 wt.% CCG, indicating successful formation of crosslinks after UV-irradiation even at high graphene contents.

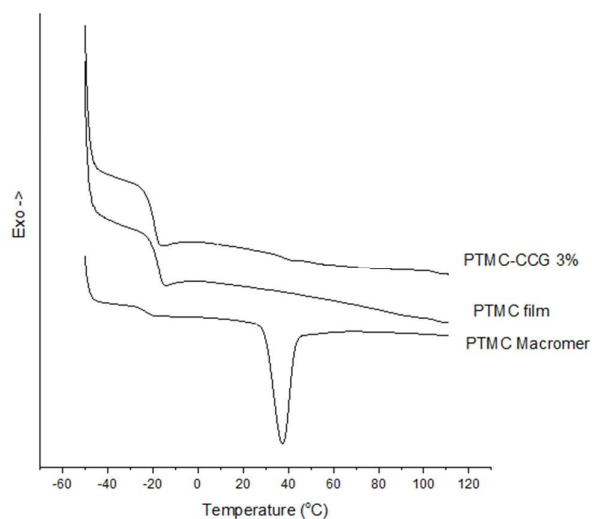


Figure S 1. Differential scanning calorimetry results for PTMC samples.

Rheological Behaviour

The apparent viscosity values of PTMC and PTMC-CCG macromers (10 wt.% macromer in DMF or DMF dispersed graphene) were plotted as a function of shear rate (Figure S 2). A

significant increase was observed in the viscosity of the PTMC on addition of graphene even at the low concentration of 0.5 wt.%, which could be related to the physical interactions between the graphene sheets and the polymer chains.¹ Apart from increasing the viscosity, a transition from liquid-like to solid-like behaviour was observed in the samples containing graphene, which could be due to graphene-graphene as well as graphene-matrix interactions. PTMC macromer shows a Newtonian behaviour with a viscosity that is much less dependent on the shear rate compared to that of the composites. In contrast, the composites showed a profound shear thinning behaviour that started from low shear rates. This non-Newtonian behaviour of the composites is due to orientation of graphene sheets in the polymer matrix below the shear force that can disturb the chain entanglements of the matrix.^{2,3} At higher shear rates, the viscosity of the composites becomes shear rate-independent due to reduction of polymer chain entanglements and decreases in viscosity caused by the increasing shear rate.

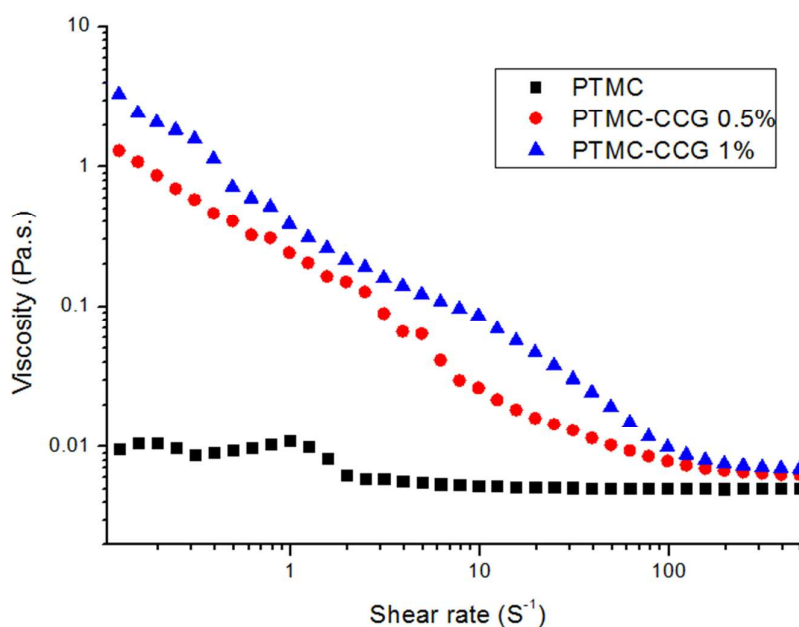


Figure S 2. Viscosity vs. shear rate for PTMC and PTMC-CCG macromers.

Electrical performance of the electrical stimulation set up

As previously described by Richardson et al.⁴, the change in impedance of the system can be derived from potential changes during the applied current pulses. Changes in the impedance of the electrode surface can be calculated from the polarization potential V_p as according to $Z_p = V_p/i$. No notable changes in V_p were observed during ES. Hence, as current was kept constant, Z_p did not change during the experiments.

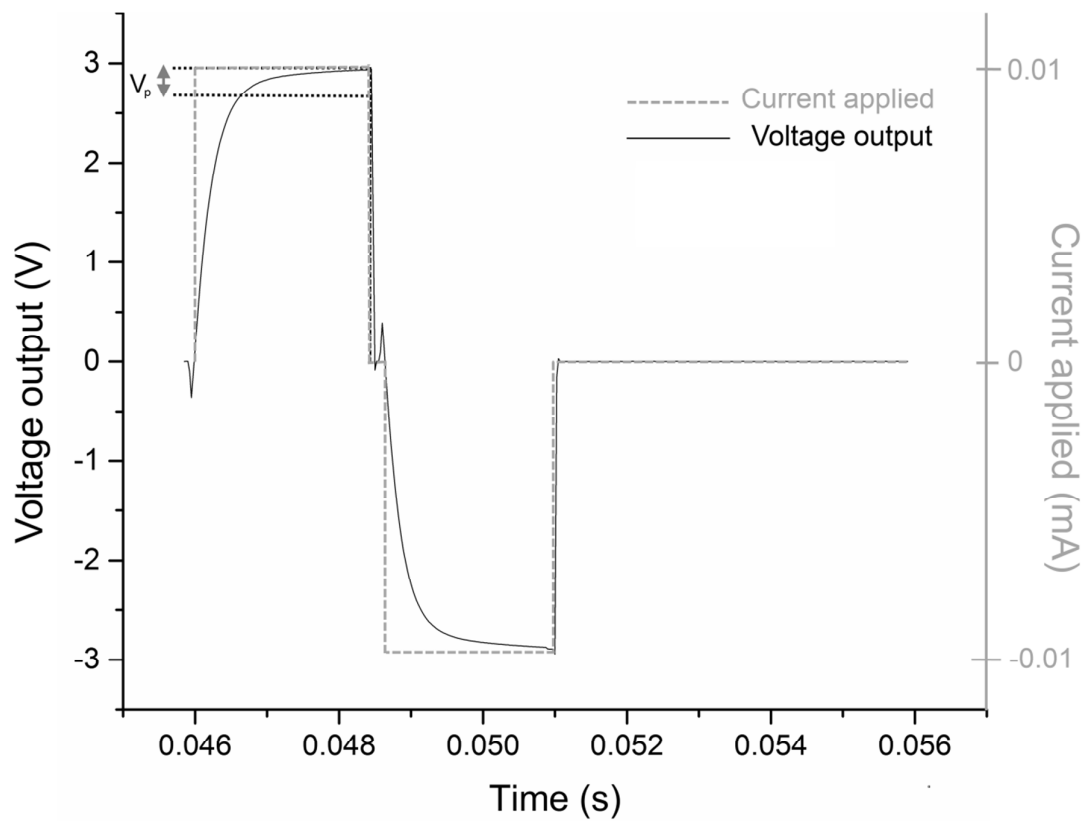


Figure S 3. An example of the waveform used and the resulting voltage for stimulating cells.

Cell number

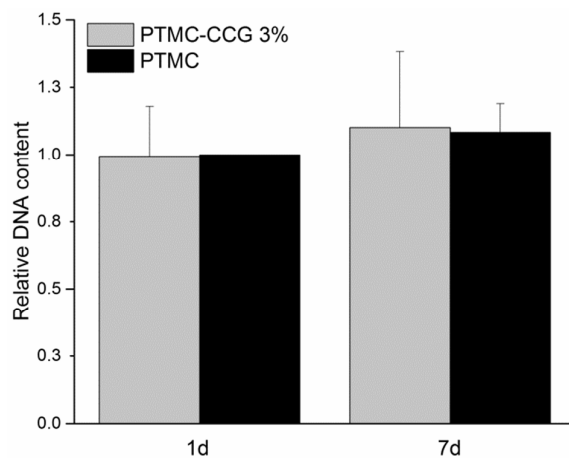


Figure S 4. Relative DNA content of MSCs on the cast films after 7 days of culture.

Flow cytometric characterisation of cell surface antigens

Table S-1. The average surface protein expression profile of MSCs characterized from all donors.

Antigen	Surface protein	Mean	SD
CD14	Serum lipopolysaccharide binding protein	0.7	0.4
CD19	B lymphocyte-lineage differentiation antigen	0.4	0.2
CD34	Sialomucin-like adhesion molecule	22.1	28.9
CD45	Leukocyte common antigen	1.1	0.2
CD73	Ecto-50-nucleotidase	94.8	3.4
CD90	Thy-1 (T cell surface glycoprotein)	99.0	0.7
CD105	SH-2, endoglin	98.7	0.9
HLA-DR	Major histocompatibility class II antigens	0.8	0.5

Primer sequences for RT-PCR

Table S-2. The primer sequences used in this study.

Primer	Sequence	Accession number
ALP	f-CCCCCGTGGCAACTCTATCT r-GATGGCAGTGAAGGGCTTCTT	NM_000478.4
Col I	f-CCAGAAGAAGTGGTACATCAGCAA r-CGCCATACTCGAACTGGAATC	NM_00088
Runx2	f-CTTCATTCGCCTCACAAACAAC r-TCCTCCTGGAGAAAGTTTGCA	NM_001024630.3
aVEGF	f-ATCAAACCTCACCAAGGCCAG r-AATGCTTTCTCCGCTCTGAGC	NM (a)

(a) Splice variants NM_001287044.1, NM_001033756.2, NM_001025369.2, NM_001025368.2, NM_001025367.2, NM_003376.5, NM_001025366.2

References

- (1) Abdel-Goad, M.; Potschke, P.; Zhou, D.; Mark, J. E.; Heinrich, G., Preparation and Rheological Characterization of Polymer Nanocomposites Based on Expanded Graphite. *J. Macromol. Sci., Part. A: Pure. Appl. Chem.* **2007**, *44* (6), 591-598.
- (2) Kim, H.; Macosko, C. W., Processing-Property Relationships of Polycarbonate/Graphene Composites. *Polymer* **2009**, *50* (15), 3797-3809.
- (3) Kharchenko, S. B.; Douglas, J. F.; Obrzut, J.; Grulke, E. A.; Migler, K. B., Flow-Induced Properties of Nanotube-Filled Polymer Materials. *Nat. Mater.* **2004**, *3* (8), 564-568.
- (4) Richardson, R. T.; Thompson, B.; Moulton, S.; Newbold, C.; Lum, M. G.; Cameron, A.; Wallace, G.; Kapsa, R.; Clark, G.; O'Leary, S., The Effect of Polypyrrole with Incorporated Neurotrophin-3 on the Promotion of Neurite Outgrowth from Auditory Neurons. *Biomaterials* **2007**, *28* (3), 513-523.